]

High temperature superconductivity due to the long-range electron-phonon interaction, application to isotope effects, thermomagnetic transport and nanoscale heterogeneity in cuprates.

A.S. Alexandrov[1]

[1] *Department of Physics, Loughborough University, Loughborough LE11 3TU, UK*

Abstract

Strong electron-phonon interactions in cuprates and other high-temperature superconductors have gathered support over the last decade in a large number of experiments. Here I briefly introduce the Fröhlich-Coulomb multi-polaron model of high-temperature superconductivity, which includes strong on-site repulsive correlations and the long-range Coulomb and electron-phonon (e-ph) interactions. Our extension of the BCS theory to the strong-coupling regime with the long-range *unscreened* electron-phonon interaction could naturally explain isotope effects, unconventional thermomagnetic transport, and checkerboard modulations of the tunnelling density of states in cuprates.

PACS numbers: PACES: 74.72.-h, 74.20.Mn, 74.20.Rp, 74.25.Dw

I. INTRODUCTION: THE FRÖHLICH-COULOMB MODEL

A significant fraction of research in the field of high-temperature superconductivity [1, 2] suggests that the interaction in novel superconductors is essentially repulsive and unretarted, but it provides high T_c without any phonons. A motivation for this concept can be found in the earlier work by Kohn and Luttinger [3], who showed that the Cooper pairing of repulsive fermions is possible. However, the same work showed that T_c of repulsive fermions is extremely low, well below the mK scale. Nevertheless, the BCS and BCS-like theories (including the Kohn-Luttinger consideration) heavily rely on the Fermi-liquid model of the *normal* state. This model fails in cuprates, so that there are no obvious *a priory* reasons to discard the dogma, if the normal state is not the Fermi-liquid. Strong onsite repulsive correlations (Hubbard U) are essential in undoped (parent) cuprates, which are *insulators* with the optical gap about $2eV$ or so. Indeed, if repulsive correlations are weak, one would expect a metallic behaviour of a half-filled d-band of copper, or, at most, a much smaller gap caused by lattice and spin distortions (i.e. charge and/or spin density waves [4]). It is a strong onsite repulsion of d-electrons which results in the "Mott" insulating state of parent cuprates. Different from conventional band-structure insulators with completely filled or empty Bloch bands, the Mott insulator arises from a potentially metallic half-filled band as a result of the Coulomb blockade of electron tunnelling to neighboring sites [5].

However, independent of any experimental evidence the Hubbard U (or $t-J$) model shares an inherent difficulty in determining the order. While some groups claimed that it describes high-T_c superconductivity at finite doping, other authors could not find any superconducting instability without an additional (i.e. e-ph) interaction [6]. Therefore it has been concluded that models of this kind are highly conflicting and confuse the issue by exaggerating the magnetism rather than clarifying it [7]. There is another serious problem with the Hubbard-U approach to high temperature superconductivity in cuprates. The characteristic (magnetic) interaction, which *might* be responsible for the pairing in the Hubbard model, is the spin exchange interaction, $J = 4t^2/U$, of the order of 0.1 eV. It turns out much smaller than the (inter-site) Coulomb repulsion and the unscreened long-range (Fröhlich) e-ph interaction each of the order of 1 eV, routinely neglected within the approach. There is virtually no screening of e-ph interactions with $c-$axis polarized optical phonons in cuprates because the upper limit for the out-of-plane plasmon frequency ($\lesssim 200$ cm^{-1})[8] is well below the

characteristic phonon frequency, $\omega \approx 400$ - 1000 cm $^{-1}$. As a result of poor screening, the magnetic interaction remains small compared with the Fröhlich interaction at any doping. Hence, any realistic approach to superconductivity and heterogeneity in cuprates should treat the Coulomb and *unscreened* e-ph interactions on an equal footing.

We have developed a so-called "Fröhlich-Coulomb" model [9, 10] to deal with the strong Coulomb and long-range e-ph interactions in cuprates and other doped oxides. The model Hamiltonian explicitly includes the long-range electron-phonon and Coulomb interactions as well as the kinetic and deformation energies. The implicitly present large Hubbard term prohibits double occupancy and removes the need to distinguish fermionic spins. Introducing spinless fermionic, $c_{\mathbf{n}}$, and phononic, $d_{\mathbf{m}\alpha}$, operators the Hamiltonian of the model is written as

$$\begin{aligned}\tilde{H} = & - \sum_{\mathbf{n}\neq\mathbf{n}'} \left[t(\mathbf{n}-\mathbf{n}') c^{\dagger}_{\mathbf{n}} c_{\mathbf{n}'} - V_c(\mathbf{n}-\mathbf{n}') c^{\dagger}_{\mathbf{n}} c_{\mathbf{n}} c^{\dagger}_{\mathbf{n}'} c_{\mathbf{n}'} \right] \\ & - \sum_{\mathbf{nm}} \omega_{\alpha} g_{\alpha}(\mathbf{m}-\mathbf{n}) (\mathbf{e}_{\alpha} \cdot \mathbf{u}_{\mathbf{m}-\mathbf{n}}) c^{\dagger}_{\mathbf{n}} c_{\mathbf{n}} (d^{\dagger}_{\mathbf{m}\alpha} + d_{\mathbf{m}\alpha}) + \sum_{\mathbf{m}\alpha} \omega_{\alpha} \left(d^{\dagger}_{\mathbf{m}\alpha} d_{\mathbf{m}\alpha} + \frac{1}{2} \right), \quad (1)\end{aligned}$$

where $\mathbf{e}_{\alpha}$ is the polarization vector of αth vibration coordinate, $\mathbf{u}_{\mathbf{m}-\mathbf{n}} \equiv (\mathbf{m}-\mathbf{n})/|\mathbf{m}-\mathbf{n}|$ is the unit vector in the direction from electron $\mathbf{n}$ to the ion $\mathbf{m}$, $g_{\alpha}(\mathbf{m}-\mathbf{n})$ is a dimensionless e-ph coupling function, and $V_c(\mathbf{n}-\mathbf{n}')$ is the inter-site Coulomb repulsion. $g_{\alpha}(\mathbf{m}-\mathbf{n})$ is proportional to the *force* acting between an electron on site $\mathbf{n}$ and an ion $\mathbf{m}$. For simplicity, we assume that all the phonon modes are non-dispersive with the frequency ω_{α}. We also use $\hbar = 1$.

The Hamiltonian, Eq.(1), can be solved analytically in the extreme case of a strong e-ph interaction where the e-ph dimensionless coupling constant is large, $\lambda = E_p/zt > 1$, by using $1/\lambda$ multipolaron expansion technique [9]. Here $E_p = \sum_{\mathbf{n}\alpha} \omega_{\alpha} g^2_{\alpha}(\mathbf{n}) (\mathbf{e}_{\alpha} \cdot \mathbf{u}_{\mathbf{n}})^2$, is the polaron level shift about 1 eV and zt is the half-bandwidth in a rigid lattice.

The model shows a reach phase diagram depending on the ratio of the inter-site Coulomb repulsion V_c and the polaron (Franc-Condon) level shift E_p [10]. The ground state is a *polaronic* Fermi liquid at large Coulomb repulsions, a *bipolaronic* high-temperature superconductor at intermediate Coulomb repulsions, and a charge-segregated insulator at weak repulsion. The model predicts *superlight* bipolarons with a remarkably high superconducting critical temperature. It describes many other properties of cuprates [9], in particular band-structure isotope effects, normal state thermomagnetic transport and real-space mod-

ulations of the single-particle density of states (DOS) as discussed below.

II. BAND-STRUCTURE ISOTOPE EFFECT

The isotope substitution, where an ion mass M is varied without any change of electronic configurations, is a powerful tool in testing the origin of electron correlations in solids. In particular, a finite value of the isotope exponent $\alpha = -d\ln T_c/d\ln M$ proved that the superconducting phase transition at $T = T_c$ is driven by the electron-phonon interaction in conventional low-temperature superconductors [11]. Advances in fabrication of isotope substituted samples made it possible to measure a sizable isotope effect also in many high-temperature superconductors. This led to a general conclusion that phonons are relevant for high T_c. Essential features of the isotope effect on T_c, in particular its large values in low T_c cuprates, an overall trend to decrease as T_c increases, and a small or even negative α in some high T_c cuprates, could be understood in the framework of the bipolaron theory of high-temperature superconductivity [12].

The most compelling evidence for (bi)polaronic carries in novel superconductors was provided by the discovery of a substantial isotope effect on the (super)carrier mass [13, 14, 15]. The effect was observed by measuring the magnetic field penetration depth λ_H of isotope-substituted copper oxides. The carrier density is unchanged with the isotope substitution of O^{16} by O^{18}, so that the isotope effect on λ_H measures directly the isotope effect on the carrier mass m^*. A carrier mass isotope exponent $\alpha_m = d\ln m^*/d\ln M$ was observed, as predicted by the bipolaron theory [12]. In ordinary metals, where the Migdal adiabatic approximation [16] is believed to be valid, $\alpha_m = 0$ is expected. However, when the e-ph interaction is sufficiently strong and electrons form polarons, their effective mass m^* depends on M as $m^* = m\exp(\gamma E_p/\omega)$. Here m is the band mass in the absence of the electron-phonon interaction, γ is a numerical constant less than 1 that depends on the radius of the electron-phonon interaction, and ω is a characteristic phonon frequency. In the expression for m^*, only the phonon frequency depends on the ion mass. Thus there is a large isotope effect on the carrier mass in (bi)polaronic conductors, $\alpha_m = (1/2)\ln(m^*/m)$ [12], in contrast with the zero isotope effect in ordinary metals.

Recent high resolution angle resolved photoemission spectroscopy (ARPES) [17] provided another compelling evidence for a strong e-ph interaction in cuprates. It revealed a fine

phonon structure in the electron self-energy of the underdoped $La_{2-x}Sr_xCuO_4$ samples [18], and a complicated isotope effect on the electron spectral function in Bi2212 [19]. Polaronic carriers were also observed in colossal magneto-resistance manganite including their low-temperature ferromagnetic phase, where the isotope effect on the residual resistivity was measured and explained [20].

These and many other experimental and theoretical observations point towards unusual e-ph interactions in complex oxides, which remain to be quantitatively addressed. We have performed quantum Monte Carlo (QMC) simulations [21] of a single-polaron problem with the long-range e-ph interaction, Eq.(1), in the most relevant intermediate region of the coupling strength, $\lambda \simeq 1$, and of the adiabatic ratio, $\omega/t \simeq 1$, where any analytical or even semi-analytical approximation (i.e. dynamic mean-field approach in finite dimensions) may fail. More recently we have calculated the isotope effect on the whole polaron band dispersion, $\epsilon_{\mathbf{k}}$, and DOS of a two-dimensional lattice polaron with short- and long-range e-ph interactions by applying the continuous-time QMC algorithm [22]. Unlike the strong-coupling limit [12] the isotope effect depends on the wave vector in the intermediate region of parameters. It also depends on the radius of the e-ph interaction. If we define a band-structure isotope exponent α_b as

$$\alpha_b \equiv -\frac{\partial \ln \epsilon_{\mathbf{k}}}{\partial \ln M}, \tag{2}$$

it does not depend on the wave-vector $\mathbf{k}$ in the extreme strong-coupling limit, $\lambda \gg 1$. E-ph interactions do not change the band topology in this limit [12], so that α_b is the same as α_m. Notwithstanding QMC results [22] show that the isotope exponent becomes a nontrivial function of the wave vector, $\alpha_b = \alpha_b(\mathbf{k})$, in the intermediate-coupling regime, because e-ph interactions substantially modify the band topology in this regime.

The isotope exponent $\alpha_b(\mathbf{k})$ are presented in Figs. (1,2), for the small Holstein polaron (SHP) with the short-range interaction, and for the small Fröhlich polaron (SFP) with the long-range interaction [22]. The polaron spectra are calculated for two phonon frequencies, $\omega = 0.70\,t$ and $\omega = 0.66\,t$, whose difference corresponds to a substitution of O^{16} by O^{18} in cuprates. There is a significant change in the dispersion law (topology) of SHP, Fig.1, which is less significant for SFP, Fig.2, rather than a simple band-narrowing. As a result, the isotope exponent, $\alpha_b(\mathbf{k}) \approx 8[\epsilon^{16}_{\mathbf{k}} - \epsilon^{18}_{\mathbf{k}}]/\epsilon^{16}_{\mathbf{k}}$, is $\mathbf{k}$-dependent, Fig.1 and Fig.2 (lower panels). The strongest dispersion of α_b is observed for SHP. Importantly, the isotope effect is suppressed near the band edge in contrast with the $\mathbf{k}$-independent strong-coupling isotope effect. It is

less dispersive for SFP, especially at larger λ.

The coherent motion of small polarons leads to metallic conduction at low temperatures. Our results, Figs.1,2 show that there should be anomalous isotope effects on low-frequency kinetics and thermodynamics of polaronic conductors which depend on the position of the Fermi level in the polaron band. Actually, such effects have been observed in ferromagnetic oxides at low temperatures [20], and in cuprates [13, 14, 15]. To address ARPES isotope exponents [19] one has to calculate the electron spectral function $A(\mathbf{k}, E)$ taking into account phonon side-bands (i.e. off diagonal transitions) along with the coherent polaron motion (diagonal transitions). Using the $1/\lambda$ expansion and a single phonon mode approximation one obtains [9]

$$A(\mathbf{k}, E) = \sum_{l=0}^{\infty} \left[A_l^{(-)}(\mathbf{k}, E) + A_l^{(+)}(\mathbf{k}, E) \right], \tag{3}$$

where

$$A_l^{(-)}(\mathbf{k}, E) = \frac{Z\left[1 - n(E - l\omega)\right]}{(2N)^l l!}$$
$$\times \sum_{\mathbf{q}_1, \ldots \mathbf{q}_l} \prod_{r=1}^{l} |\gamma(\mathbf{q}_r)|^2 \delta[E - l\omega - \xi(\mathbf{k}_l^-)],$$

and

$$A_l^{(+)}(\mathbf{k}, E) = \frac{Z \cdot n(E + l\omega)}{(2N)^l l!} \sum_{\mathbf{q}_1, \ldots \mathbf{q}_l} \prod_{r=1}^{l} |\gamma(\mathbf{q}_r)|^2 \delta[E - l\omega - \xi(\mathbf{k}_l^+)]. \tag{4}$$

Here $Z = \exp(-E_p/\omega)$, $\xi(\mathbf{k}) = \epsilon_{\mathbf{k}} - \mu$, μ is the chemical potential, $n(E) = [\exp(\beta E) + 1]^{-1}$, $\mathbf{k}_l^{\pm} = \mathbf{k} \pm \sum_{r=1}^{l} \mathbf{q}_r$ and $\gamma(\mathbf{q})$ is the Fourier transform of the force, $\gamma(\mathbf{q}) = \sqrt{2} \sum_{\mathbf{n}} g(\mathbf{n})(\mathbf{e} \cdot \mathbf{u}_{\mathbf{n}}) \exp(i\mathbf{q} \cdot \mathbf{n})$.

Clearly, Eq. (3) is in the form of a perturbation multi-phonon expansion. Each contribution $A_l^{(\pm)}(\mathbf{k}, E)$ to the spectral function describes the transition from the initial state $\mathbf{k}$ of the polaron band to the final state $\mathbf{k}_l^{\mp}$ with the emission (or absorption) of l phonons. Different from the conventional Migdal self-energy [16] the electron spectral function comprises two parts in the strong-coupling limit. The first ($l = 0$) $\mathbf{k}$-dependent term arises from the coherent polaron tunnelling, $A_{coh}(\mathbf{k}, E) = \left[A_0^{(-)}(\mathbf{k}, E) + A_0^{(+)}(\mathbf{k}, E) \right] = Z\delta(E - \zeta_{\mathbf{k}})$ with a suppressed spectral weight $Z \ll 1$. The second *incoherent* part $A_{incoh}(\mathbf{k}, E)$ comprises all terms with $l \geq 1$. It describes excitations accompanied by emission and absorption of phonons. We note that its spectral density spreads over a wide energy range of about twice the polaron level shift E_p, which might be larger than the unrenormalized bandwidth $2zt$

in the rigid lattice. On the contrary, the coherent part shows a dispersion only in the energy window of the order of the polaron bandwidth. It is important that the *incoherent* background $A_{incoh}(\mathbf{k}, E)$ could be dispersive (i.e. $\mathbf{k}$-dependent) for the long-range interaction. Only in the Holstein model with the short-range nondispersive e-ph interaction, $\gamma(\mathbf{q}) = constant$, the incoherent part has no dispersion.

Using Eq. (3) one readily predicts the isotope effect on the coherent part dispersion $\epsilon_{\mathbf{k}}$ and its spectral weight Z, *and* also on the incoherent background because Z, $\gamma(\mathbf{q})$, and ω all depend on M. While our prediction is qualitatively robust it is difficult to quantify the ARPES isotope effect in the intermediate region of parameters. The spectral function, Eq. (3), is applied in the strong-coupling limit $\lambda \gg 1$. While the main sum rule $\int_{-\infty}^{\infty} dE A(\mathbf{k}, E) = 1$ is satisfied, the higher-momentum integrals $\int_{-\infty}^{\infty} dE E^p A(\mathbf{k}, E)$ with $p > 0$, calculated with Eq. (3) differ from their exact values [23] by an amount proportional to $1/\lambda$. The difference is due to partial "undressing" of high-energy excitations in phonon side-bands, which is beyond the lowest order $1/\lambda$ expansion. The role of electronic correlations should be also addressed in connection with ARPES. While the results shown in Figs.1,2 describe band-structure isotope effects in slightly-doped conventional and Mott-Hubbard insulators with a few carriers, their spectral properties could be significantly modified by the polaron-polaron interactions [24], including the bipolaron formation [25] at finite doping. On the experimental side, separation of the coherent and incoherent parts in ARPES remains rather controversial.

III. THERMOMAGNETIC TRANSPORT

There is much evidence for the crossover regime at T^* and normal state charge and spin gaps in the cuprates [9, 26]. Within the Fröhlich-Coulomb model these energy gaps could be understood as being half of the binding energy, Δ_p, and the singlet-triplet gap of preformed bipolarons, respectively [9]. Notwithstanding some "direct" evidence for the existence of a charge $2e$ Bose liquid in the normal state of cuprates is highly desirable. Mott and Alexandrov[27] discussed the thermal conductivity κ; the contribution from the carriers given by the Wiedemann-Franz ratio depends strongly on the elementary charge as $\sim (e^*)^{-2}$ and should be significantly suppressed in the case of $e^* = 2e$ compared with the Fermi-liquid contribution. As a result, the Lorenz number, $L = (e/k_B)^2 \kappa_e/(T\sigma)$ differs

significantly from the Sommerfeld value $L_e = \pi^2/3$ of the standard Fermi-liquid theory, if carriers are bipolarons. Here κ_e, σ, and e are the electronic thermal conductivity, the electrical conductivity, and the elementary charge, respectively. Ref. [27] predicted a rather low Lorenz number L_b for bipolarons, $L_b = 6L_e/(4\pi^2) \approx 0.15L_e$, due to the double charge on bosonic carriers, and also due to their nearly classical distribution above T_c.

Unfortunately, the extraction of the electron thermal conductivity has proven difficult since both the electron term, κ_e and the phonon term, κ_{ph} are comparable to each other in the cuprates. Only recently a new way to determine the Lorenz number has been realized by Zhang et al.[28], based on the thermal Hall conductivity. The thermal Hall effect allowed for an efficient way to separate the phonon heat current even when it is dominant. As a result, the "Hall" Lorenz number, $L_H = (e/k_B)^2 \kappa_{xy}/(T\sigma_{xy})$, has been directly measured in $YBa_2Cu_3O_{6.95}$ because transverse thermal κ_{xy} and electrical σ_{xy} conductivities involve only electrons. Remarkably, the measured value of L_{xy} just above T_c is about the same as predicted by the bipolaron model, $L_{xy} \approx 0.15L_e$.

The experimental L_{xy} showed a strong temperature dependence, which violates the Wiedemann-Franz law. This experimental observation is hard to explain in the framework of any Fermi-liquid model. Based on the Fröhlich-Coulomb model and the conventional Boltzmann kinetics in the τ approximation we developed a theory of the Lorenz number in the cuprates explaining the experimental results by Zhang et al [29]. We have demonstrated that the Wiedemann-Franz law breaks down because of the interference of polaron and bipolaron contributions to the heat transport. When thermally excited polarons and also triplet pairs are included, our model explains the violation of the Wiedemann-Franz law in cuprates and the Hall Lorenz number as seen in the experiment, Fig.3.

A large Nernst signal observed *well above* the resistive critical temperature T_c provides another important piece of evidence for a qualitatively different normal state of cuprates as compared with conventional superconductors. It has been attributed to a *vortex* motion in a number of cuprates [30, 31]. As a result the magnetic phase diagram of the cuprates has been revised with the upper critical field $H_{c2}(T)$ curve not ending at T_{c0} but at much higher temperatures [31]. Most surprisingly, Ref.[31] estimated H_{c2} *at the zero-field resistive transition temperature* of Bi2212, T_{c0}, as high as 50-150 Tesla. However, any scenario with a nonzero off-diagonal order parameter (the Bogoliubov-Cor'kov anomalous average), $F(\mathbf{r}_1, \mathbf{r}_2) = \left\langle \hat{\Psi}_\downarrow(\mathbf{r}_1)\hat{\Psi}_\uparrow(\mathbf{r}_2) \right\rangle$, above T_c, such as of Ref. [31, 32], is difficult to reconcile with

the extremely sharp resistive and magnetic transitions at T_c in single crystals of cuprates. Above T_c the uniform magnetic susceptibility is paramagnetic and the resistivity is perfectly 'normal', showing only a few percent positive or negative magnetoresistivity. Both in-plane [33, 34, 35] and out-of-plane [36] resistive transitions remain sharp in the magnetic field in high quality samples providing a reliable determination of a genuine $H_{c2}(T)$.

While a significant fraction of research in the field suggests that the superconducting transition is only a phase ordering so that a superconducting order parameter $F(\mathbf{r}_1, \mathbf{r}_2)$ remains nonzero above (resistive) T_c, we have recently explained the unusual Nernst signal (which is one of the key experiments supporting that viewpoint) as the normal state phenomenon [37].

Cuprates are known to be non-stoichiometric compounds. Moreover, undoped cuprates are insulators and their superconductivity appears as a result of doping, which inevitably introduces additional disorder. Because of these reasons, the theory of doped semiconductors might provide an adequate description of the normal state kinetic properties of cuprates. Carriers in doped semiconductors and disordered metals occupy states localised by disorder and itinerant Bloch-like states. Both types of carriers contribute to the transport properties, if the chemical potential μ (or the Fermi level) is close to the energy, where the lowest itinerant state appears (i.e. to the mobility edge). Superconducting cuprates are among such poor conductors.

When the chemical potential is near the mobility edge, and the effective mass approximation is applied, there is no Nernst signal from itinerant carriers alone, because of a so-called Sondheimer cancellation [38]. However, when the localised carriers contribute to the longitudinal transport, a finite positive Nernst signal $e_y \equiv -E_y/\nabla_x T$ appears as [37]

$$\frac{e_y}{\rho} = \frac{k_B}{e} r\theta\sigma_l, \tag{5}$$

where $\rho = 1/[(2s+1)\sigma_{xx}]$ is the resistivity, s is the carrier spin, r is about a constant ($r{\approx}14.3$ for fermions $s{=}1/2$, $r{\approx}2.4$ for bosons $s{=}0$), and Θ is the Hall angle. Here σ_{xx} is the conductivity of itinerant carriers above the mobility edge, and σ_l is the conductivity of localised carriers below the edge, which obeys the Mott's law, $\sigma_l = \sigma_0 \exp\left[-(T_0/T)^{1/3}\right]$ (σ_0 is about a constant). In two dimensions $T_0 \approx 8\alpha^2/(k_B N_l)$, where N_l is the DOS at the Fermi level[39, 40, 41].

In sufficiently strong magnetic field the radius of a shallow 'impurity' state α^{-1} is about

the magnetic length, $\alpha \approx (eB)^{1/2}$. Then the normal state Nernst signal is given by

$$\frac{e_y}{B\rho} = a(T) \exp\left[-b(B/T)^{1/3}\right], \tag{6}$$

where $a(T) \propto T^{-6}$ [37] and $b = 2[e/(k_B N_l)]^{1/3}$ is a constant. As shown in Ref. [37] a single-parameter Eq.(6) is in excellent quantitative agreement with the experimental data [30, 31] above the resistive critical temperature $T_c(B)$, Fig.4.

As far as statistics of carriers is concerned, the bipolaron or 'preformed boson' picture is strongly supported by many other data in underdoped and optimally doped cuprates [9], while overdoped cuprates might be on the Fermi-liquid side. Unlike any fluctuating preformed pair scenario, eg. [43], bosons in our model are perfectly stable, and there is no off-diagonal order above their Bose condensation temperature, T_c, There is no off-diagonal order parameter above T_c in the overdoped Fermi-liquid either. In both cases the localization of carriers by disorder is essential. It is responsible for the strong Nernst signal dependence on the magnetic field, Fig.4. It can be also responsible for a low value of the product of the thermopower and the Hall angle $S \tan\Theta$ in some underdoped samples, where the contribution to the thermopower from itinerant carriers can be almost cancelled by the opposite sign contribution from the localised carriers, so that $S \propto T$ at low temperatures. For two-dimensional bosons it is feasible even if $\sigma_{xx} \gg \sigma_l$[37]. When it happens, the Nernst signal is given by $e_y = \rho\alpha_{xy}$, where $\alpha_{xy} \propto \tau^2$. Different from that of fermions, the relaxation time of bosons is enhanced critically near the Bose-Einstein condensation temperature, $T_c(B)$, $\tau \propto [T - T_c(B)]^{-1/2}$, as in atomic Bose-gases [44]. Providing $S \tan\Theta_H \ll e_y$, this critical enhancement of the relaxation time describes well the temperature dependence of e_y in a few Bi2201 close to $T_c(B)$.

Superconductivity can be readily suppressed by the magnetic field in heavily underdoped cuprates to reveal a true normal state down to zero temperature. The normal state in-plane resistivity $\rho(T)$ shows an insulating behaviour at low temperatures, which has been understood as the result of elastic (impurity) scattering of nondegenerate carriers above the mobility edge [45]. Combining $\rho(T) \propto 1/\tau$, $S \tan\Theta \propto T\tau$, and $e_y + S \tan\Theta \propto \tau$ one obtains

$$S \tan\Theta \propto \frac{T}{\rho(T)}, \tag{7}$$

and

$$e_y \propto \frac{T_0 - T}{\rho(T)}, \tag{8}$$

where T_0 is a fitting parameter. I believe that Eq.(7) and Eq.(8) can account for the experimental Nernst and $S \tan \Theta$ data in underdoped $La_{1.92}Sr_{0.08}CuO_4$ [46] and $La_{1.94}Sr_{0.06}CuO_4$ [47] with the field-induced insulating behaviour of $\rho(T)$. The unusual large Nernst signal appears due to the absence of the electron-hole symmetry near the mobility edge in the transverse transport. Our results strongly support any microscopic theory of cuprates, which describes the state above the resistive and magnetic phase transition as perfectly 'normal', $F(\mathbf{r}, \mathbf{r}')$=0. Unlike [31], our model does not require a radical revision of the magnetic phase diagram of cuprates [42]. Also an unusual diamagnetic response of underdoped cuprates experimentally measured somewhat above $T_c(B)$ [48, 49, 50] can be understood as the Landau diamagnetism of *normal* state bosons [51].

IV. CHECKERBOARD MODULATIONS OF TUNNELLING DOS

There are more complicated deviations from the conventional Fermi/BCS-liquid behaviour than the normal state pseudogaps. Recent studies of the gap function revealed two distinctly different gaps with different magnetic field and temperature dependence [52, 53, 54], and the checkerboard spatial modulations of the tunnelling DOS, with [55] and without [56, 57] applied magnetic fields.

We have proposed a simple phenomenological model [58] explaining two different gaps in cuprates. The main assumption, supported by a parameter-free estimate of the Fermi energy [59], is that the attractive potential is large compared with the renormalised Fermi energy, so that the ground state is the Bose-Einstein condensate of tightly bound real-space pairs. Here I calculate the single particle DOS of strong-coupling (bosonic) superconductors by solving the inhomogeneous Bogoliubov-de Genes (BdG) equations [60].

The anomalous Bogoliubov-Gor'kov average $F(\mathbf{r}_1, \mathbf{r}_2)$ depends on the relative coordinate $\rho = \mathbf{r}_1 - \mathbf{r}_2$ of two electrons (holes), described by field operators $\hat{\Psi}_s(\mathbf{r})$, and on the center-of-mass coordinate $\mathbf{R} = (\mathbf{r}_1 + \mathbf{r}_2)/2$. Its Fourier transform, $f(\mathbf{k}, \mathbf{K})$, depends on the relative momentum $\mathbf{k}$ and on the center-of-mass momentum $\mathbf{K}$. In the BCS theory $\mathbf{K}$ =0, and the Fourier transform of the order parameter is proportional to the gap in the quasi-particle excitation spectrum, $f(\mathbf{k}, \mathbf{K}) \propto \Delta_{\mathbf{k}}$. Hence the symmetry of the order parameter and the symmetry of the gap are the same in the weak-coupling regime. Under the rotation of the coordinate system, $\Delta_{\mathbf{k}}$ changes its sign, if the Cooper pairing appears in the d-channel.

On the other hand, the symmetry of the order parameter could be different from the 'internal' symmetry of the pair wave-function, and from the symmetry of a single-particle excitation gap in the strong-coupling regime [9]. Real-space pairs might have an unconventional symmetry due to a specific symmetry of the pairing potential as in the case of the Cooper pairs, but in any case the ground state and DOS are homogeneous, if pairs are condensed with $\mathbf{K} = 0$. However, if a pair band dispersion has its minima at finite $\mathbf{K}$ in the center-of-mass Brillouin zone, the Bose condensate is inhomogeneous. In particular, the center-of-mass bipolaron energy bands could have their minima at the Brillouin zone boundaries at $\mathbf{K} = (\pi, 0)$ and three other equivalent momenta [61] (here and further I take the lattice constant $a = 1$). These four states are degenerate, so that the condensate wave function $\psi(\mathbf{m})$ in the real (Wannier) space, $\mathbf{m} = (m_x, m_y)$, is their superposition,

$$\psi(\mathbf{m}) = \sum_{\mathbf{K}=(\pm\pi,0),(0,\pm\pi)} b_{\mathbf{K}} e^{-i\mathbf{K}\cdot\mathbf{m}}, \tag{9}$$

where $b_{\mathbf{K}} = \pm\sqrt{n_c}/2$ are c-numbers, and $n_c(T)$ is the atomic density of the Bose-condensate. The superposition, Eq.(9), respects the time-reversal and parity symmetries, if

$$\psi(\mathbf{m}) = \sqrt{n_c}\left[\cos(\pi m_x) \pm \cos(\pi m_y)\right]. \tag{10}$$

The order parameter, Eq.(10), has d-wave symmetry changing sign in the real space, when the lattice is rotated by $\pi/2$. This symmetry is entirely due to the pair-band energy dispersion with four minima at $\mathbf{K} \neq 0$, rather than due a specific pairing potential. It reveals itself as a *checkerboard* modulation of the hole density with two-dimensional patterns, oriented along the diagonals. From this insight one can expect a fundamental connection between stripes detected by different techniques [62] and the symmetry of the order parameter in cuprates [61].

Now let us take into account that in the superconducting state ($T < T_c$) single-particle excitations interact with the pair condensate via the same attractive potential, which forms the pairs [58]. The Hamiltonian describing the interaction of excitations with the pair Bose-condensate in the Wannier representation is

$$H = -\sum_{s,\mathbf{m},\mathbf{n}} [t(\mathbf{m}-\mathbf{n}) + \mu\delta_{\mathbf{m},\mathbf{n}}] c^{\dagger}_{s\mathbf{m}} c_{s\mathbf{n}} + \sum_{\mathbf{m}} [\Delta(\mathbf{m}) c^{\dagger}_{\uparrow\mathbf{m}} c_{\downarrow\mathbf{m}} + H.c.], \tag{11}$$

where $s = \uparrow, \downarrow$ is the spin, and $\Delta(\mathbf{m}) \propto \psi(\mathbf{m})$. Applying equations of motion for the

Heisenberg operators $\tilde{c}^{\dagger}_{s\mathbf{m}}(t)$ and $\tilde{c}_{s\mathbf{m}}(t)$, and the Bogoliubov transformation [63]

$$\tilde{c}_{\uparrow\mathbf{m}}(t) = \sum_{\nu}[u_{\nu}(\mathbf{m})\alpha_{\nu}e^{-i\epsilon_{\nu}t} + v^{*}_{\nu}(\mathbf{m})\beta^{\dagger}_{\nu}e^{i\epsilon_{\nu}t}], \tag{12}$$

$$\tilde{c}_{\downarrow\mathbf{m}}(t) = \sum_{\nu}[u_{\nu}(\mathbf{m})\beta_{\nu}e^{-i\epsilon_{\nu}t} - v^{*}_{\nu}(\mathbf{m})\alpha^{\dagger}_{\nu}e^{i\epsilon_{\nu}t}], \tag{13}$$

one obtains BdG equations describing the single-particle excitation spectrum,

$$\epsilon u(\mathbf{m}) = -\sum_{\mathbf{n}}[t(\mathbf{m}-\mathbf{n}) + \mu\delta_{\mathbf{m},\mathbf{n}}]u(\mathbf{n}) + \Delta(\mathbf{m})v(\mathbf{m}), \tag{14}$$

$$-\epsilon v(\mathbf{m}) = -\sum_{\mathbf{n}}[t(\mathbf{m}-\mathbf{n}) + \mu\delta_{\mathbf{m},\mathbf{n}}]v(\mathbf{n}) + \Delta(\mathbf{m})u(\mathbf{m}), \tag{15}$$

where excitation quantum numbers ν are omitted for transparency. Different from the conventional BdG equations in the weak-coupling limit, there is virtually no feedback of single particle excitations on the off-diagonal potential, $\Delta(\mathbf{m})$, in the strong-coupling regime. The number of these excitations is low at temperatures below Δ_p/k_B, so that the coherent potential $\Delta(\mathbf{m})$ is an external (rather than a self-consistent) field, solely determined by the pair Bose condensate [58].

While the analytical solution is not possible for any arbitrary off-diagonal interaction $\Delta(\mathbf{m})$, one can readily solve the infinite system of discrete equations (14,15) for a periodic $\Delta(\mathbf{m})$ with a period commensurate with the lattice constant. For example,

$$\Delta(\mathbf{m}) = \Delta_c[e^{i\pi m_x} - e^{i\pi m_y}], \tag{16}$$

corresponds to the pair condensate at $\mathbf{K} = (\pm\pi, 0)$ and $(0, \pm\pi)$, Eq.(10), with a temperature dependent (coherent) $\Delta_c \propto \sqrt{n_c(T)}$. In this case the quasi-momentum $\mathbf{k}$ is the proper quantum number, $\nu = \mathbf{k}$, and the excitation wave-function is a superposition of plane waves,

$$u_{\nu}(\mathbf{m}) = u_{\mathbf{k}}e^{i\mathbf{k}\cdot\mathbf{m}} + \tilde{u}_{\mathbf{k}}e^{i(\mathbf{k}-\mathbf{g})\cdot\mathbf{m}}, \tag{17}$$

$$v_{\nu}(\mathbf{m}) = v_{\mathbf{k}}e^{i(\mathbf{k}-\mathbf{g}_x)\cdot\mathbf{m}} + \tilde{v}_{\mathbf{k}}e^{i(\mathbf{k}-\mathbf{g}_y)\cdot\mathbf{m}}. \tag{18}$$

Here $\mathbf{g}_x = (\pi, 0)$, $\mathbf{g}_y = (0, \pi)$, and $\mathbf{g} = (\pi, \pi)$ are reciprocal doubled lattice vectors. Substi-

tuting Eqs.(17) and (18) into Eqs.(14,15) one obtains four coupled algebraic equations,

$$\epsilon_{\mathbf{k}} u_{\mathbf{k}} = \xi_{\mathbf{k}} u_{\mathbf{k}} - \Delta_c(v_{\mathbf{k}} - \tilde{v}_{\mathbf{k}}), \tag{19}$$

$$\epsilon_{\mathbf{k}} \tilde{u}_{\mathbf{k}} = \xi_{\mathbf{k}-\mathbf{g}} \tilde{u}_{\mathbf{k}} + \Delta_c(v_{\mathbf{k}} - \tilde{v}_{\mathbf{k}}), \tag{20}$$

$$-\epsilon_{\mathbf{k}} v_{\mathbf{k}} = \xi_{\mathbf{k}-\mathbf{g}_x} v_{\mathbf{k}} + \Delta_c(u_{\mathbf{k}} - \tilde{u}_{\mathbf{k}}), \tag{21}$$

$$-\epsilon_{\mathbf{k}} \tilde{v}_{\mathbf{k}} = \xi_{\mathbf{k}-\mathbf{g}_y} \tilde{v}_{\mathbf{k}} - \Delta_c(u_{\mathbf{k}} - \tilde{u}_{\mathbf{k}}), \tag{22}$$

where $\xi_{\mathbf{k}} = -\sum_{\mathbf{n}} t(\mathbf{n}) e^{i\mathbf{k}\cdot\mathbf{n}} - \mu$. The determinant of the system (19-22) yields the following equation for the energy spectrum ϵ:

$$\begin{aligned} &(\epsilon - \xi_{\mathbf{k}})(\epsilon - \xi_{\mathbf{k}-\mathbf{g}})(\epsilon + \xi_{\mathbf{k}-\mathbf{g}_x})(\epsilon + \xi_{\mathbf{k}-\mathbf{g}_y}) \\ &= \Delta_c^2 (2\epsilon + \xi_{\mathbf{k}-\mathbf{g}_x} + \xi_{\mathbf{k}-\mathbf{g}_y})(2\epsilon - \xi_{\mathbf{k}} - \xi_{\mathbf{k}-\mathbf{g}}). \end{aligned} \tag{23}$$

Two positive roots for ϵ describe the single-particle excitation spectrum. Their calculation is rather cumbersome, but not in the extreme strong-coupling limit, where the pair binding energy $2\Delta_p$ is large compared with Δ_c and with the single-particle bandwidth w. The chemical potential in this limit is pinned below a single-particle band edge, so that $\mu = -(\Delta_p + w/2)$ is negative, and its magnitude is large compared with Δ_c. Then the right hand side in Eq.(23) is a perturbation, and the spectrum is

$$\epsilon_{1\mathbf{k}} \approx \xi_{\mathbf{k}} - \frac{\Delta_c^2}{\mu}, \tag{24}$$

$$\epsilon_{2\mathbf{k}} \approx \xi_{\mathbf{k}-\mathbf{g}} - \frac{\Delta_c^2}{\mu}, \tag{25}$$

If a metallic tip is placed at the point $\mathbf{m}$ above the surface of a sample, the STM current $I(V, \mathbf{m})$ creates an electron (or hole) at this point. Applying the Fermi-Dirac golden rule and the Bogoliubov transformation, Eq.(12,13), and assuming that the temperature is much lower than Δ_p/k_B one readily obtains the tunnelling conductance

$$\sigma(V, \mathbf{m}) \equiv \frac{dI(V, \mathbf{m})}{dV} \propto \sum_{\nu} |u_\nu(\mathbf{m})|^2 \delta(eV - \epsilon_\nu), \tag{26}$$

which is a local excitation DOS. The solution Eq.(17) leads to a spatially modulated conductance,

$$\sigma(V, \mathbf{m}) = \sigma_{reg}(V) + \sigma_{mod}(V) \cos(\pi m_x + \pi m_y). \tag{27}$$

The smooth (regular) contribution is

$$\sigma_{reg}(V) = \sigma_0 \sum_{\mathbf{k}, r=1,2} (u_{r\mathbf{k}}^2 + \tilde{u}_{r\mathbf{k}}^2) \delta(eV - \epsilon_{r\mathbf{k}}), \tag{28}$$

and the amplitude of the modulated contribution is

$$\sigma_{mod}(V) = 2\sigma_0 \sum_{\mathbf{k},r=1,2} u_{r\mathbf{k}}\tilde{u}_{r\mathbf{k}}\delta(eV - \epsilon_{r\mathbf{k}}), \tag{29}$$

where σ_0 is a constant. Conductance modulations reveal a checkerboard pattern, as the Bose condensate itself, Eq.(10),

$$\frac{\sigma - \sigma_{reg}}{\sigma_{reg}} = A\cos(\pi m_x + \pi m_y), \tag{30}$$

where

$$A = 2\sum_{\mathbf{k}} \left[u_{1\mathbf{k}}\tilde{u}_{1\mathbf{k}}\delta(eV - \epsilon_{1\mathbf{k}}) + u_{2\mathbf{k}}\tilde{u}_{2\mathbf{k}}\delta(eV - \epsilon_{2\mathbf{k}})\right] / \\ \sum_{\mathbf{k}} \left[(u^2_{1\mathbf{k}} + \tilde{u}^2_{1\mathbf{k}})\delta(eV - \epsilon_{1\mathbf{k}}) + (\tilde{u}^2_{2\mathbf{k}} + u^2_{2\mathbf{k}})\delta(eV - \epsilon_{2\mathbf{k}})\right]$$

is the amplitude of modulations depending on the voltage V and temperature. An analytical result can be obtained in the strong-coupling limit with the excitation spectrum given by Eqs. (24,25) for the voltage near the threshold, $eV \approx \Delta_p$. In this case only states near bottoms of each excitation band contribute to the integrals in Eq.(30), so that

$$\tilde{u}_{1\mathbf{k}} = \frac{\xi_{\mathbf{k}} - \epsilon_{1\mathbf{k}}}{\epsilon_{1\mathbf{k}} - \xi_{\mathbf{k}-\mathbf{g}}} u_{1\mathbf{k}} \approx -u_{1\mathbf{k}}\frac{\Delta_c^2}{\mu w} \ll u_{1\mathbf{k}}, \tag{31}$$

and

$$u_{2\mathbf{k}} = \frac{\xi_{\mathbf{k}-\mathbf{g}} - \epsilon_{2\mathbf{k}}}{\epsilon_{2\mathbf{k}} - \xi_{\mathbf{k}}} \tilde{u}_{2\mathbf{k}} \approx -\tilde{u}_{2\mathbf{k}}\frac{\Delta_c^2}{\mu w} \ll \tilde{u}_{2\mathbf{k}}. \tag{32}$$

Substituting these expressions into A, Eq.(30), yields in the lowest order of Δ_c,

$$A \approx -\frac{2\Delta_c^2}{\mu w}. \tag{33}$$

The result, Eq.(30), is reminiscent of STM data [55, 56, 57, 64], where spatial checkerboard modulations of σ were observed in a few cuprates. Both commensurate and incommensurate modulations were found depending on sample composition. In our model the period is determined by the center-of mass wave vectors $\mathbf{K}$ of the Bose-condensed preformed pairs. While the general case has to be solved numerically, the perturbation result, Eq.(30) is qualitatively applied for any $\mathbf{K}$ at least close to T_c, where the coherent gap is small, if one replaces $\cos(\pi m_x + \pi m_y)$ by $\cos(K_x m_x + K_y m_y)$. Different from any other scenario, proposed so far, the hole density, which is about twice of the condensate density at low temperatures, is spatially modulated with the period determined by the inverse wave vectors corresponding to

the center-of-mass pair band-minima. This 'kinetic' interpretation of charge modulations in cuprates was originally proposed [61] before STM results became available. It could account for those DOS modulations in superconducting samples, which disappear above T_c because the coherent gap $\Delta_c(T)$ vanishes, so that $A = 0$ in Eq.(30). Indeed some inelastic neutron scattering experiments show that incommensurate inelastic peaks are observed *only* in the *superconducting* state of high-T_c cuprates [65]. The vanishing at T_c of incommensurate peaks is inconsistent with any other stripe picture, where a characteristic distance needs to be observed in the normal state as well. On the other hand some STM studies (see, for example [66]) report incommensurate and commensurate DOS modulations somewhat above T_c, in particular, in heavily underdoped cuprates [67]. I believe that those modulations are due to a single-particle band structure and impurity states near the top of the valence band in doped charge-transfer insulators, rather than a signature of any cooperative phenomenon.

In conclusion, the strong-coupling Fröhlich-Coulomb model, Eq.(1), links charge heterogeneity, pairing, and pseudo-gaps as manifestations of the strong electron-phonon attractive interaction in narrow bands of doped Mott-Hubbard insulators.

The author acknowledges support of this work by the Leverhulme Trust (London) Grant No. F/00261/H , The Royal Society, and by EPSRC (UK) Grant No. EP/C518365/1.

---

[1] P.W. Anderson, *The Theory of Superconductivity in the High T_c Cuprates* (Princeton University Press, Princeton, 1997).

[2] E.W. Carlson, V.J. Emery, S.A. Kivelson, and D. Orgad, in *The Physics of Superconductors*, Vol.2, eds. K.H. Bennemann and J.B. Ketterson (Springer-Verlag, NY, 2004).

[3] W. Kohn and J.M. Luttinger, Phys. Rev. Lett. **15**, 524 (1965).

[4] A.M. Gabovich, A.I. Voitenko, J.F. Annett, and M. Ausloos, 2001 Supercond. Sci. Technol. **14**, R1 (2001).

[5] N.F. Mott, *Metal-Insulator Transitions, 2nd ed.* (Taylor&Francis, London, 1990).

[6] A. Scherman and M. Scrieber, Phys. Rev. B**52**, 10621 (1995).

[7] R.B. Laughlin, cond-mat/0209269.

[8] J.H. Kim, B.J. Feenstra, H.S. Somal, D. van der Marel, W.Y. Lee, A.M. Gerrits, and A. Wittlin, Phys. Rev. B**49**, 13065 (1994).

[9] A.S. Alexandrov, *Theory of Superconductivity: from Weak to Strong Coupling* (IoP Publishing, Bristol-Philadelphia, 2003).

[10] A.S. Alexandrov and P.E. Kornilovitch, J. Phys.: Condens. Matter **14**, 5337 (2002).

[11] E. Maxwell, Phys. Rev. **78**, 477 (1950); C. A. Reynolds, B. Serin, W. H. Wright, and L. B. Nesbitt, ibid 487 (1950).

[12] A.S. Alexandrov, Phys. Rev. B**46**, 14932 (1992).

[13] G. Zhao and D. E. Morris, Phys. Rev. B **51**, 16487 (1995).

[14] G. Zhao, M.B. Hunt, H. Keller, and K.A. Müller, Nature **385**, 236 (1997).

[15] R. Khasanov, D.G. Eshchenko, H. Luetkens, E. Morenzoni, T. Prokscha, A. Suter, N. Garifianov, M. Mali, J. Roos, K. Conder, and H. Keller, Phys. Rev. Lett. **92**, 057602 (2004).

[16] A.B. Migdal, Zh. Eksp. Teor. Fiz. **34**, 1438 (1958) (Sov. Phys. JETP **7**, 996 (1958)).

[17] A. Lanzara, P.V. Bogdanov, X.J. Zhou, S.A. Kellar, D.L. Feng, E.D. Lu, T. Yoshida, H. Eisaki, A. Fujimori, K. Kishio, J.I. Shimoyana, T. Noda, S. Uchida, Z. Hussain, and Z.X. Shen, Nature **412**, 510 (2001).

[18] X.J. Zhou, J. Shi, T. Yoshida, T. Cuk, W. L. Yang, V. Brouet, J. Nakamura, N. Mannella, S. Komiya, Y. Ando, F. Zhou, W. X. Ti, J. W. Xiong, Z. X. Zhao, T. Sasagawa, T. Kakeshita, H. Eisaki, S. Uchida, A. Fujimori, Zhenyu Zhang, E. W. Plummer, R. B. Laughlin, Z. Hussain, and Z.-X. Shen, cond-mat/0405130.

[19] G-H. Gweon, T. Sasagawa, S.Y. Zhou, J. Craf, H. Takagi, D.-H. Lee, and A. Lanzara, Nature, **430**, 187 (2004).

[20] A. S. Alexandrov, G.-m. Zhao, H. Keller, B. Lorenz, Y. S. Wang, and C. W. Chu, Phys. Rev. B **64**, 140404(R) (2001).

[21] A.S. Alexandrov and P.E. Kornilovitch, Phys. Rev. Lett. **82**, 807 (1999).

[22] A.S. Alexandrov and P.E. Kornilovitch, Phys. Rev. B**70**, 224511 (2004).

[23] P.E. Kornilovitch, EuroPhys. Lett. **59**, 735 (2002).

[24] J. Tempere and J.T. Devreese, Phys. Rev. B **64**, 104504 (2001).

[25] A.S. Alexandrov and C.J. Dent, Phys. Rev. B **60**, 15414 (1999).

[26] T. Timusk and B. Statt, Rep. Prog. Phys. **62**, 61 (1999).

[27] A.S. Alexandrov and N.F. Mott, Phys. Rev. Lett, **71**, 1075 (1993).

[28] Y. Zhang, N.P. Ong, Z.A. Xu, K. Krishana, R. Gagnon, and L. Taillefer, Phys. Rev. Lett., **84**, 2219 (2000).

[29] K.K. Lee, A.S. Alexandrov and W.Y. Liang, Phys. Rev. Lett. **90**, 217001 (2003); ibid, Eur. Phys. J. B**39**, 459 (2004).

[30] Y. Wang, S. Ono, Y. Onose, G. Gu, Y. Ando, Y. Tokura, S. Uchida, N.P. Ong, Science **299**, 86 (2003).

[31] Y. Wang, N.P. Ong, Z.A. Xu, T. Kakeshita, S. Uchida, D.A. Bonn, R. Liang, W.N. Hardy, Phys. Rev. Lett. **88**, 257003 (2002).

[32] V.J. Emery, S.A. Kivelson, Nature, **374**, 434 (1995).

[33] A.P. Mackenzie, S.R. Julian, G.G. Lonzarich, A. Carrington, S.D. Hughes, R.S. Liu, D.C. Sinclair, Phys. Rev. Lett. **71**, 1238 (1993)

[34] M.S. Osofsky, R. J. Soulen, S.A. Wolf, J.M. Broto, H. Rakoto, J.C. Ousset, G. Coffe, S. Askenazy, P. Pari, I. Bozovic, J.N. Eckstein, G. F. Virshup, Phys. Rev. Lett. **71**, 2315 (1993); ibid **72**, 3292 (1994).

[35] D.D. Lawrie, J.P. Franck, J.R. Beamish, E.B. Molz, W.M. Chen, M.J. Graft, J. Low Temp. Phys. **107**, 491 (1997).

[36] A.S. Alexandrov, V.N. Zavaritsky, W.Y. Liang, P.L. Nevsky, Phys. Rev. Lett. **76** 983 (1996).

[37] A. S. Alexandrov and V. N. Zavaritsky Phys. Rev. Lett. **93** 217002 (2004).

[38] E.H. Sondheimer, Proc. Roy. Soc. **193**, 484 (1948).

[39] N.F. Mott, and E.A. Davis, *Electronic Processes in Non-Crystalline Materials* (Clarendon Press,Oxford, 1979).

[40] B.I. Shklovskii, Soviet Phys. JETP Lett. **36**, 51 (1982).

[41] R. Mansfield and H. Tokumoto, Phil Mag. B**48**, L1 (1983).

[42] A.S. Alexandrov, Phys. Rev. B **48**, 10571 (1993); V.N. Zavaritsky, V.V. Kabanov, and A.S. Alexandrov, Europhys. Lett. **60**, 127, (2002).

[43] S. Tan and K. Levin, Phys.Rev. B 69, 064510 (2004).

[44] T. Lopez-Arias and A. Smerzi, Phys. Rev. A **58**, 526 (1998).

[45] A.S. Alexandrov, Phys. Lett. A**236**, 132 (1997).

[46] C. Capan, K. Behnia, J. Hinderer, A.G.M. Jansen, W. Lang, C. Marcenat, C. Marin, and J. Flouquet, Phys. Rev. Lett. **88**, 056601 (2002).

[47] C. Capan and K. Behnia, cond-mat/0501288.

[48] R. Jin, A. Schilling, and H. R. Ott, Phys. Rev. B 49, 9218 (1994).

[49] A. Sugimoto, I. Iguchi, T. Miyake, and H. Sato, Japanise Journal of Applied Physics, **41**,

L497 (2002).

[50] Y. Wang, Lu Li, M. J. Naughton, G. D. Gu, S. Uchida, and N. P. Ong, cond-mat/0503190.

[51] C.J. Dent, A.S. Alexandrov and V.V. Kabanov Physica C**341**, 153 (2000).

[52] G. Deutscher, Nature **397**, 410 (1999).

[53] V. M. Krasnov, A. Yurgens, D. Winkler, P. Delsing, and T. Claeson, Phys. Rev. Lett. **84**, 5860 (2000).

[54] J. Demsar, R. Hudej, J. Karpinski, V. V. Kabanov, and D. Mihailovic, Phys. Rev. B **63**, 054519 (2001).

[55] J. E. Hoffman, E. W. Hudson, K. M. Lang, V. Madhavan, H. Eisaki, S. Uchida, and J. C. Davis, Science **295**, 466 (2002).

[56] J. E. Hoffman, K. McElroy, D.-H. Lee, K. M Lang, H. Eisaki, S. Uchida, and J. C. Davis, Science **297**, 1148 (2002).

[57] C. Howald, H. Eisaki, N. Kaneko, M. Greven, and A. Kapitulnik, Phys. Rev. B**67**, 014533 (2003).

[58] A.S. Alexandrov and A.F. Andreev, Europhys. Lett. **54**, 373 (2001).

[59] A.S. Alexandrov, Physica C **363**, 231 (2001).

[60] A.S. Alexandrov, cond-mat/0407401.

[61] A.S. Alexandrov, Physica C **305**, 46 (1998).

[62] A. Bianconi, J. Phys. IV France **9**, 325 (1999), and references therein.

[63] N. Bogoliubov, J.Phys. USSR **11**, 23 (1947).

[64] for an experimental summary see H.C. Fu, J.C. Davis and D.-H Lee, cond-mat/0403001.

[65] P. Bourges, Y. Sidis, H. F. Fong, L. P. Regnault, J. Bossy, A. Ivanov, and B. Keimer, Science, **288** 1234 (2000); J. Supercond. **13**, 735 (2000).

[66] M. Vershinin, S. Misra, S. Ono, Y. Abe, Y. Ando, and A. Yazdani, Science **303**, 1995 (2004).

[67] T. Hanaguri, C. Lupien, Y. Kohsaka, D. -H. Lee, M. Azuma, M. Takano, H. Takagi, and J. C. Davis, cond-mat/0409102.

Figure captions:

Fig.1. Top panels: small Holstein polaron band dispersions along the main directions of the two-dimensional Brillouin zone. Left: $\lambda = 1.1$, right: $\lambda = 1.2$. Filled symbols is $\omega = 0.70\,t$, open symbols is $\omega = 0.66\,t$. Lower panels: the band structure isotope exponent for $\lambda = 1.1$ (left) and $\lambda = 1.2$ (right).

Fig.2. Top panels: small Fröhlich polaron band dispersions along the main directions of the two-dimensional Brillouin zone. Left: $\lambda = 2.5$, right: $\lambda = 3.0$. Filled symbols is $\omega = 0.70\,t$, open symbols is $\omega = 0.66\,t$. Lower panels: the band structure isotope exponent for $\lambda = 2.5$ (left) and $\lambda = 3.0$ (right).

Fig.3. The Hall Lorenz number L_H [29] fits the experiment ($YBa_2Cu_3O_{6.95}$ [28]). Charge and spin pseudogaps are taken as 675 K and 150 K, respectively, and the ratio of the polaron and bipolaron Hall angles is 0.36. The inset gives the ratio of Hall Lorenz number to Lorenz number in the model.

Fig.4. Eq.(6) fits the experimental signal (symbols) in overdoped $La_{1.8}Sr_{0.2}CuO_4$ [31] with $b = 7.32(\mathrm{K/Tesla})^{1/3}$. Inset shows $a(T)$ obtained from the fit (dots) together with $a \propto T^{-6}$ (line).

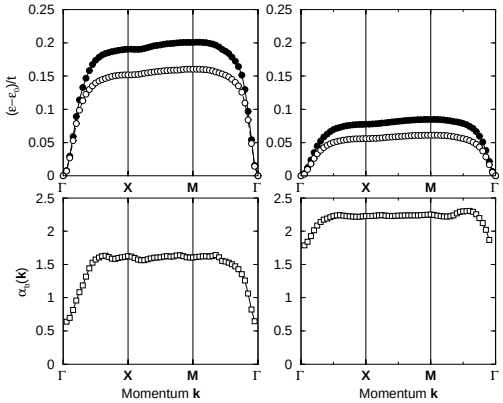

FIG. 1:

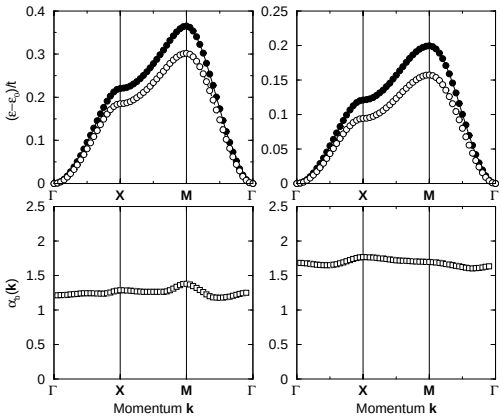

FIG. 2:

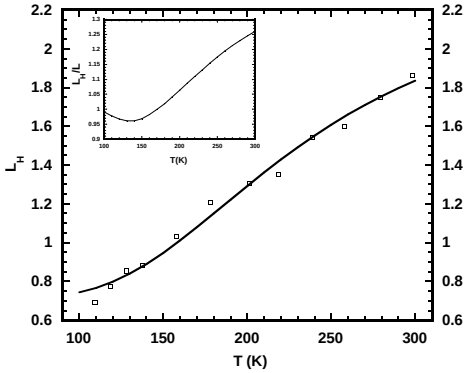

FIG. 3:

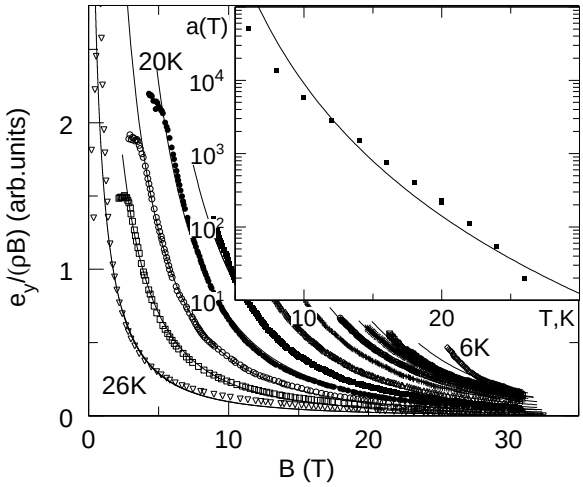

FIG. 4: